International Journal of Innovative
Computing, Information and Control
Volume **16**, Number **6**, December **2020**

 ISSN 1349-4198
pp. **1959–1971**

CALCULATION METHOD FOR WAVELENGTH PATH PLANNING IN ARRAYED WAVEGUIDE GRATING – STAR NETWORK

Minoru Yamaguchi, Osanori Koyama, Kanami Ikeda and Makoto Yamada

Graduate School of Engineering
Osaka Prefecture University
Gakuen-cho 1-1, Naka-ku, Sakai, Osaka 599-8531, Japan
m.yamaguchi@m.ieice.org; { koyama; kanami; myamada }@eis.osakafu-u.ac.jp

Received July 2020; revised October 2020

Abstract. *In our previous study, we proposed an arrayed waveguide grating – STAR network with a loopback function to avoid traffic congestion and inefficient utilization of wavelength path capacity. The proposed network can relocate wavelength paths in response to traffic demand by controlling simple optical switches. However, the network management of the proposed method seems complicated because of the change in the wavelength path topology and fluctuation of its accumulated optical loss due to wavelength path relocation. Therefore, we previously proposed a calculation method that is suitable for the AWG-STAR network with a loopback function to solve the issue that it is difficult to manage a reconfigurable network. The proposed method enables network operators to easily calculate and manage the dynamic relocatable wavelength path topology. However, it cannot calculate the transit nodes and the accumulated optical loss along each wavelength path. In this paper, we propose a method for calculating the wavelength path and signal power. The proposed method expressed network topology so that this method could also calculate network information based on topologies such as distance and latency and be helpful for a network controller that needs topology information. The proposed method minimizes the operating expenses for complex networks by clarifying path relations among nodes.*

Keywords: Networked control systems, Path planning, Wavelength routing

1. **Introduction.** Recently, telecommunications traffic has been growing rapidly. In this regard, wavelength division multiplexing (WDM) is adopted for networks to increase traffic capacity. In addition, the traffic demand in data centers has been growing rapidly as well. Data center networks are required to have low power consumption, low delay, scalability, and flexibility. Reconfigurable optical add-drop multiplexers (ROADMs) have been developed to efficiently and flexibly allocate wavelength paths in WDM networks. Moreover, the introduction of arrayed waveguide grating routers (AWGRs) in data centers has been proposed [1,2]. The importance of AWGRs has been increasing in relatively small-scale networks. It has been proposed to reconfigure the topology by establishing directly path between top of rack (ToR) switches to mitigate hotspots in data center providing large-scale social media services. c-Through [3] and Helios [4] are hybrid methods for reconfiguring the path topology that use both electrical and optical switching. Helios has the functions of path reconfiguration and traffic arrangement on the switch side, and c-Through has these functions on the server-side. REACToR [5] is also a hybrid method that enables flexible traffic control by synchronizing packet switching and optical burst switching. ProjecToR [6] is one of the solutions using free-space optics with a digital micromirror device which enables high-capacity communication and high-speed switching.

DOI: 10.24507/ijicic.16.06.1959

In our previous study, we proposed a network architecture that can relocate a wavelength path based on Ethernet by using AWGR and inexpensive optical switches for relatively small-scale networks. This is because the wavelength path topology of the arrayed waveguide grating (AWG) – STAR network is generally fixed despite fluctuations in traffic demands [7]. Figure 1 shows a schematic of the proposed network. The figure shows how the nodes and AWGR are connected. The nodes comprise a multiplexer (MUX), a demultiplexer (DEMUX), OSWs corresponding to each wavelength, and a layer-3 switch (L3SW) that can transmit WDM signals. MUX/DEMUX is needed to connect the WDM network and L3SW with colored interfaces. OSWs are important components that enable reconfiguring the topology by switching an optical path from connection with AWGR and L3SW to connection with the output port and input port of AWGR. Flexible optical path relocation by OSW before L3SW's routing enables low latency and efficient capacity utilization. The signals transmitted from the nodes are inputted to the AWGR. These signals are routed to each of the output ports following the wavelength routing characteristics of the AWGR. The signals routed by the AWGR are received at each node when the state of the OSW is C_{PT} and inputted again to the AWGR by looping back the signal when the state of the OSW is C_{LB}, as shown in Figure 1. Consequently, the optical path is relocated by routing the signal again. Figure 1 shows an example that a 4×4 AWGR and three wavelengths are used. In this case, λ_1 in node 2 and λ_3 in node 4 are looped-back and the others are path through and so the number of wavelength paths from node 3 to node 1 is increased three. Furthermore, we demonstrated that the multiple wavelength paths could be dynamically relocated in the proposed AWG-STAR network [8-11]. However, the wavelength path relocation in the proposed AWG-STAR network makes the wavelength path topology complex, thus making it extremely difficult to manage wavelength path and network capacity. A calculation method for wavelength path topology using a wavelength transfer matrix was proposed for an AWG-STAR network with fixed wavelength path topology [12,13]. However, the calculation method in [12,13] cannot be directly applied to the proposed AWG-STAR network. This is because it cannot express the relocation of a specific wavelength path. Therefore, we proposed a calculation method that is suitable for the AWG-STAR network with a loopback function [14]. The proposed method enables network operators to easily calculate and manage the dynamic relocatable wavelength path topology. However, it cannot calculate the transit nodes and the accumulated optical loss along each wavelength path. Meanwhile, the method proposed in [14] can be used to obtain the node connectivity and the number of paths. The calculation method can only represent the relationship between the input and output of the number of paths. This is because the elements of the matrices are represented as only "1" or "0" corresponding to whether wavelength signals can pass through the corresponding route or not. Moreover, whether the wavelength paths can be established or not is determined based on whether the calculation result obtained by multiplying all the elements passing through is "1" or "0", similar to the AND gate in a logical circuit. It is very important to accurately manage the optical loss because the reachability of the wavelength path is strongly related to transit nodes and optical loss [15]. The accumulated optical loss depends on the transit nodes and the length of the optical fiber in each wavelength path. Furthermore, the accumulated optical loss determines the flexibility of the wavelength path relocation [16]. Therefore, to maintain the capability for data communication, the network operator must control the optical loss corresponding to transit nodes and the optical fiber included in the wavelength path.

In this paper, we propose a generalized calculation method based on [14] that can determine the wavelength paths that include the transit nodes. The proposed method is different from the previous method [14]. The calculation method is generalized using

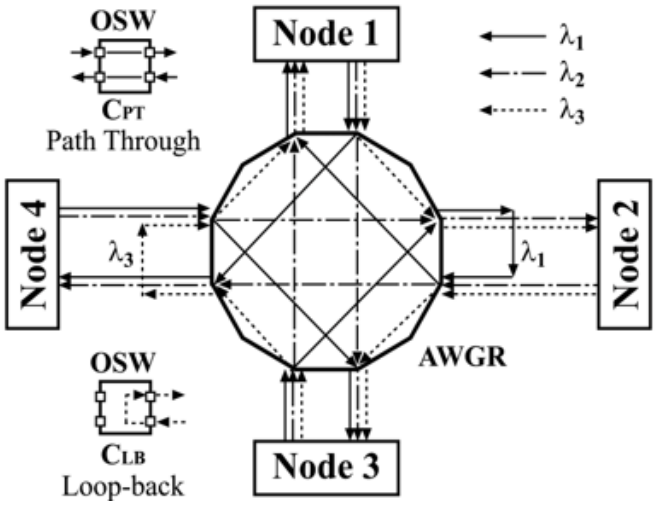

FIGURE 1. Scheme of AWG-STAR network with loopback function

variable not binary digits; the previous method represents only the result of whether a signal is through or not (1 or 0), whereas the proposed method represents variables that are multiplied by all the entries passing through. Consequently, the proposed method can determine the wavelength paths that include the transit nodes. Moreover, various calculations can be executed by substituting values regarding path information. In Section 2, we propose a new calculation method for the wavelength path relocation, so we explain the calculation method and meaning and usage of the output matrix. In this explanation, the previous method [14] is one of the applications of the proposed generalized calculation method. In Section 3, we show concrete examples by applying the proposed calculation method to a network configured using a 4×4 AWGR to confirm the applicability of the proposed matrix calculation method. Finally, we summarize the results of this research in Section 4.

2. **Description of the Matrix Calculation Method.** In this section, we describe the proposed calculation method that can calculate a path topology that includes transit nodes and optical margins. Target networks include AWGR, MUX/DEMUX, and OSW. When the number of nodes in the AWG-STAR network was n, the $\boldsymbol{O}$, $\boldsymbol{S}$, $\boldsymbol{L}$, and $\boldsymbol{I}$ matrices had n rows and n columns. Additionally, the number of wavelengths used in the AWG-STAR network was n because the wavelength paths were constructed by multiplexing n wavelengths. Here, $\boldsymbol{I}$, $\boldsymbol{O}$, and $\boldsymbol{S}$ represent the characteristics of the input wavelength from the nodes to the AWGR, the relationship between the connection nodes and wavelength paths, and the state of an OSW, respectively. Each element $i_{p,q}$, $o_{j,k}$, and $s_{p,q}$ is, respectively, expressed as follows:

$$\boldsymbol{I} = (i_{p,q}) \quad \begin{matrix} p = 1, \ldots, n\text{: node number} \\ q = 1, \ldots, n\text{: wavelength number} \end{matrix} \tag{1}$$

$$\boldsymbol{O} = (o_{j,k}) \quad \begin{matrix} j = 1, \ldots, n\text{: source node number} \\ k = 1, \ldots, n\text{: destination node number} \end{matrix} \tag{2}$$

$$\boldsymbol{S} = (s_{p,q}) \quad \begin{matrix} p = 1, \ldots, n\text{: node number} \\ q = 1, \ldots, n\text{: wavelength number} \end{matrix} \tag{3}$$

where $i_{p,q}$ is the wavelength path of λ_q inputted from node p to AWGR, $o_{j,k}$ is the number of wavelength paths transmitted from nodes j to k, and $s_{p,q}$ is the state of an OSW installed in node p to control λ_q. When the state of the OSW was $\mathrm{C_{PT}}$, $s_{p,q}$ was 0; when

the state of OSW was C_{LB}, $s_{p,q}$ was 1. Here, $\boldsymbol{L}$ represents the wavelength transfer matrix. The $\boldsymbol{L}$ rows were source nodes and the $\boldsymbol{L}$ columns were destination nodes. The entry Λ_r of $\boldsymbol{L}$ indicated a wavelength routed by the routing function of the AWGR. In this study, the AWGR exhibited a cyclic characteristic. Therefore, $\boldsymbol{L}$ and its entries can be expressed as follows:

$$\boldsymbol{L} = \begin{pmatrix} \Lambda_1 & \Lambda_2 & \Lambda_3 & \cdots & \Lambda_r & \cdots & \Lambda_n \\ \Lambda_n & \Lambda_1 & \Lambda_2 & \cdots & \Lambda_{r-1} & \cdots & \Lambda_{n-1} \\ \Lambda_{n-1} & \Lambda_n & \Lambda_1 & \cdots & \Lambda_{r-2} & \cdots & \Lambda_{n-2} \\ \vdots & \vdots & \vdots & \vdots & \vdots & \ddots & \vdots \\ \Lambda_2 & \Lambda_3 & \Lambda_4 & \cdots & \Lambda_{r+1} & \cdots & \Lambda_1 \end{pmatrix} \quad r = 1, 2, \ldots, n \tag{4}$$

where r is the entry number of $\boldsymbol{L}$. It is necessary to confirm prior to calculation whether the relationship between $\boldsymbol{I}$ and $\boldsymbol{S}$ is contradictory. When the state of the OSW of λ_q in node p was C_{LB}, the signal of λ_q transmitted from L3SW in node p was looped back through the OSW and λ_q was not inputted into the AWGR. Thus, the matrix entry $i_{p,q}$ of $\boldsymbol{I}$ had to be 0. To confirm this, we define the detection matrix $\boldsymbol{D}$ as follows:

$$\boldsymbol{D} = \boldsymbol{I} \circ \boldsymbol{S} = (d_{p,q}) \quad \begin{array}{l} p = 1, \ldots, n\text{: node number} \\ q = 1, \ldots, n\text{: wavelength number} \end{array} \tag{5}$$

where matrix entries $d_{p,q}$ were determined by multiplying $i_{p,q}$ and $s_{p,q}$. When $d_{p,q}$ was not 0, it was observed that the signal of λ_q in node p was not inputted into the AWGR as it was looped back to L3SW. Thus, entries of $\boldsymbol{I}$ or $\boldsymbol{S}$ were changed, with the result that $\boldsymbol{D}$ was 0. The calculation of path topology that includes transit nodes was performed for a matrix corresponding to each wavelength; next, $\boldsymbol{I_q}$, $\boldsymbol{S_q}$, and $\boldsymbol{L_q}$ were calculated.

First, the $\boldsymbol{I_q}$ corresponding to λ_q was calculated from $\boldsymbol{I}$. The $\boldsymbol{I_q}$ is expressed as follows:

$$\boldsymbol{I_q} = diag(i_{1,q}, i_{2,q}, \ldots, i_{n,q}) \tag{6}$$

Equation (6) indicates $\boldsymbol{I_q}$, which is created by converting each diagonal element of an $n \times n$ identity matrix into each element $(i_{p,q})$ of the column corresponding to λ_q of $\boldsymbol{I}$. In the same manner, each $\boldsymbol{L_q}$ based on $\boldsymbol{L}$ was calculated. Thus, the $\boldsymbol{L_q}$ corresponding to λ_q and the element $l_{j,k}$ of $\boldsymbol{L_q}$ can be expressed as follows:

$$\boldsymbol{L_q} = (l_{j,k}) \quad \begin{array}{l} j = 1, \ldots, n\text{: source node number} \\ k = 1, \ldots, n\text{: destination node number} \end{array} \tag{7}$$

$$l_{j,k} = \begin{cases} l_{j,k}, & q = r \\ 0, & q \neq r \end{cases} \tag{8}$$

The OSW state matrix $\boldsymbol{S_q}$ and its entries $t_{j,k}$ are expressed as follows:

$$\boldsymbol{S_q} = (t_{j,k}) \tag{9}$$

$$t_{j,k} = \begin{cases} e_{m,j}, & s_{p,q} = 0 \\ l_{j,m}, & s_{p,q} = 1 \end{cases}, \quad m = 1, 2, \ldots, n \tag{10}$$

Equation (10) shows that the m-th column of $\boldsymbol{S_q}$ was equal to the m-th column of the identity matrix when the state of the OSW of λ_q in node m was C_{PT}. Alternatively, Equation (10) shows that the m-th column of $\boldsymbol{S_q}$ was equal to the m-th row of $\boldsymbol{L_q}$, when the state of the OSW was C_{LB}. Here, $\boldsymbol{O_q}$ corresponding to λ_q is expressed as follows:

$$\boldsymbol{O_q} = (o_{j,k}) \quad \begin{array}{l} j = 1, \ldots, n\text{: source node number} \\ k = 1, \ldots, n\text{: destination node number} \end{array} \tag{11}$$

and $\boldsymbol{O_q}$ is calculated using Equation (12):

$$\boldsymbol{O_q} = \left(\boldsymbol{S_q^z} \cdot (\boldsymbol{L_q})^T \cdot \boldsymbol{I_q}\right)^T \tag{12}$$

where z is the loopback number and $\boldsymbol{S_q^z}$ is an identity matrix if z is 0. T denotes the operation of matrix transposition. Finally, $\boldsymbol{O}$ is calculated as follows:

$$\boldsymbol{O} = \sum_{q=1}^{n} \boldsymbol{O_q} \tag{13}$$

where the element $o_{j,k}$ in $\boldsymbol{O}$ indicates the path topology of the AWG-STAR network and exhibits the source, transit, and destination nodes by multiplication of $i_{p,q}$ and $l_{j,k}$. The polynomial expression of $o_{j,k}$ that comprises the multiplication terms $i_{p,q}$ and $l_{j,k}$ shows path information between nodes j and k. For example, the wavelength path from node 1 to node 3 was a direct path when $o_{j,k}$ was $i_{1,3}l_{1,3}$. Similarly, when $o_{j,k}$ was $i_{1,2}l_{1,2}l_{2,3} + i_{1,3}l_{1,3}$, we obtain two wavelength paths, namely: one direct path from nodes 1 to 3 and a loopback path from nodes 1 to 3, transiting through node 2. Therefore, the proposed calculation method can show network topology including transit nodes. Furthermore, the polynomial expression of $o_{j,k}$ showed path capacity or signal power by substituting capacity and power or loss thereof for $i_{p,q}$ and $l_{j,k}$. We observed that when path capacity and "1" were substituted for elements $i_{p,q}$ and $l_{j,k}$, respectively, $\boldsymbol{O}$ was obtained as path capacity. Previous method [14] could calculate only this capacity and could not express transit nodes. However, the proposed method can calculate more network information such as signal power and optical margins and express the transit nodes, in addition to the functions the previous method already had. When the transmitting power (mW) and optical loss (antilogarithm value) were substituted for elements $i_{p,q}$ and $l_{j,k}$, respectively, $\boldsymbol{O_q}$ was calculated as the receiving power (mW). The substituted values of $i_{p,q}$ were the transmitting power passed OSW, and the substituted values of $l_{j,k}$ were the optical loss passed MUX/DEMUX, AWGR, MUX/DEMUX, and OSW. The value of $i_{p,q}$ was 0 mW whenever the transceiver was not transmitted. When the $\boldsymbol{O_q}$ was converted from unit mW to dBm, the matrix of optical margins $\boldsymbol{M_q}$ corresponding to λ_q was calculated as follows:

$$\boldsymbol{M_q} = \boldsymbol{O_q} - \min P \tag{14}$$

where $\min P$ is the minimum light reception power of the optical transceiver. When J_q was above 0, the wavelength path was available. Alternatively, when it was below 0, the wavelength path was not available. The calculation for optical margin can judge whether wavelength path can be established or not. We showed calculation for capacity, optical power, and optical margin but these applications were one of the applications. Proposed method basically expressed network topology so that this method could also calculate network information based on topology such as distance and latency and be helpful for network controller that need topology information.

3. **Calculation Example.** In this section, we use two concrete examples to illustrate the proposed matrix calculation method. Figure 2 shows the proposed AWG-STAR network experimentally using a 4×4 AWGR. The loopback function can be implemented using a simple 2×2 optical switch and MUX/DEMUX. Here, a wavelength selective switch (WSS) was used. This is because when the number of optical switches needed for each wavelength increases, the physical configuration becomes more complex. The loopback wavelengths and passed-through signals were connected to MUX and DEMUX, respectively. The MUX multiplexed the L3SW transmit signals and the loopback signal. In addition, it sent an optical signal to the node. Meanwhile, the DEMUX split the passed-through signal and received the optical signal at the L3SW.

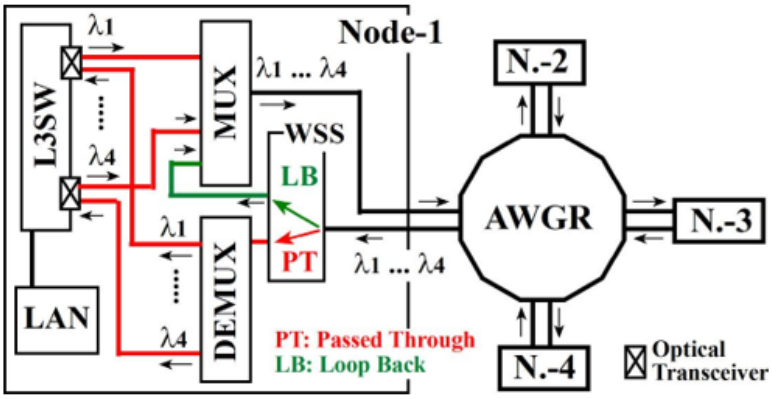

FIGURE 2. (color online) Physical configuration of AWG-STAR network with loopback function

Table 1 shows the wavelength routing characteristics of a 4×4 AWGR. In the initial state, the nodes were assumed to be logically connected wavelength paths with a full-mesh topology.

TABLE 1. Wavelength routing table in a 4×4 AWGR

AWGR port	Out-1	Out-2	Out-3	Out-4
In-1	λ_1	λ_2	λ_3	λ_4
In-2	λ_4	λ_1	λ_2	λ_3
In-3	λ_3	λ_4	λ_1	λ_2
In-4	λ_2	λ_3	λ_4	λ_1

For the first example, we made some changes to the wavelength path topology and network capacity of the network by switching the states of the OSW corresponding to λ_2 in nodes 3 and 4 from C_{PT} to C_{LB}.

First, we expressed the initial state as a full-mesh path topology in the experimental network with the proposed matrix representation. The wavelength transfer matrix $\boldsymbol{L}$ was expressed as follows:

$$\boldsymbol{L} = \begin{pmatrix} \Lambda_1 & \Lambda_2 & \Lambda_3 & \Lambda_4 \\ \Lambda_4 & \Lambda_1 & \Lambda_2 & \Lambda_3 \\ \Lambda_3 & \Lambda_4 & \Lambda_1 & \Lambda_2 \\ \Lambda_2 & \Lambda_3 & \Lambda_4 & \Lambda_1 \end{pmatrix}.$$

As eight wavelengths from all the nodes were initially inputted into a WRC, the input matrix $\boldsymbol{I}$ and the OSW state matrix $\boldsymbol{S}$ were expressed as follows (because all the OSWs were C_{PT}).

$$\boldsymbol{I} = \begin{pmatrix} i_{1,1} & i_{1,2} & i_{1,3} & i_{1,4} \\ i_{2,1} & i_{2,2} & i_{2,3} & i_{2,4} \\ i_{3,1} & i_{3,2} & i_{3,3} & i_{3,4} \\ i_{4,1} & i_{4,2} & i_{4,3} & i_{4,4} \end{pmatrix}, \quad \boldsymbol{S} = \begin{pmatrix} 0 & 0 & 0 & 0 \\ 0 & 0 & 0 & 0 \\ 0 & 0 & 0 & 0 \\ 0 & 0 & 0 & 0 \end{pmatrix}.$$

Therefore, the detection matrix $\boldsymbol{D}$ was a zero matrix. Thus, all signals could be inputted into WRC. Here, $\boldsymbol{O}$ was calculated as follows:

$$\boldsymbol{O} = \sum_{q=1}^{4} \boldsymbol{O_q} = \begin{pmatrix} i_{1,1}l_{1,1} & i_{1,2}l_{1,2} & i_{1,3}l_{1,3} & i_{1,4}l_{1,4} \\ i_{2,4}l_{2,1} & i_{2,1}l_{2,2} & i_{2,2}l_{2,3} & i_{2,3}l_{2,4} \\ i_{3,3}l_{3,1} & i_{3,4}l_{3,2} & i_{3,1}l_{3,3} & i_{3,2}l_{3,4} \\ i_{4,2}l_{4,1} & i_{4,3}l_{4,2} & i_{4,4}l_{4,3} & i_{4,1}l_{4,4} \end{pmatrix}.$$

Consequently, the nodes were obtained to be logically connected wavelength paths with a full-mesh topology.

Then, we show the matrix calculation for wavelength path relocation. When the states of the OSW corresponding to λ_2 in nodes 3 and 4 from C_{PT} to C_{LB} were changed, then the $\boldsymbol{S}$ and $\boldsymbol{D}$ matrices were expressed as follows:

$$\boldsymbol{S} = \begin{pmatrix} 0 & 0 & 0 & 0 \\ 0 & 0 & 0 & 0 \\ 0 & 1 & 0 & 0 \\ 0 & 1 & 0 & 0 \end{pmatrix}, \ \boldsymbol{D} = \begin{pmatrix} 0 & 0 & 0 & 0 \\ 0 & 0 & 0 & 0 \\ 0 & i_{3,2} & 0 & 0 \\ 0 & i_{4,2} & 0 & 0 \end{pmatrix}.$$

In this case, we found that the wavelengths λ_2 in nodes 3 and 4 could not input into the WRC. Therefore, we stopped transmitting the signals corresponding to λ_2 in nodes 3 and 4. Accordingly, $\boldsymbol{I}$ was expressed as:

$$\boldsymbol{I} = \begin{pmatrix} i_{1,1} & i_{1,2} & i_{1,3} & i_{1,4} \\ i_{2,1} & i_{2,2} & i_{2,3} & i_{2,4} \\ i_{3,1} & 0 & i_{3,3} & i_{3,4} \\ i_{4,1} & 0 & i_{4,3} & i_{4,4} \end{pmatrix}.$$

We proceed to the next calculation as the detection matrix $\boldsymbol{D}$ was 0. The $\boldsymbol{I_2}$, $\boldsymbol{L_2}$, and $\boldsymbol{S_2}$ matrices were expressed as follows:

$$\boldsymbol{I_2} = \begin{pmatrix} i_{1,2} & 0 & 0 & 0 \\ 0 & i_{2,2} & 0 & 0 \\ 0 & 0 & 0 & 0 \\ 0 & 0 & 0 & 0 \end{pmatrix}, \ \boldsymbol{L_2} = \begin{pmatrix} 0 & l_{1,2} & 0 & 0 \\ 0 & 0 & l_{2,3} & 0 \\ 0 & 0 & 0 & l_{3,4} \\ l_{4,1} & 0 & 0 & 0 \end{pmatrix}, \ \boldsymbol{S_2} = \begin{pmatrix} 1 & 0 & 0 & 0 \\ 0 & 1 & l_{2,3} & 0 \\ 0 & 0 & 0 & l_{3,4} \\ 0 & 1 & 0 & 0 \end{pmatrix}.$$

Thus, $\boldsymbol{O_2}$ corresponding to wavelength 7 was expressed as the following equation:

$$\boldsymbol{O_2} = \left(\boldsymbol{S_2^2} \cdot (\boldsymbol{L_2})^T \cdot \boldsymbol{I_2}\right)^T = \begin{pmatrix} 0 & i_{1,2}l_{1,2} & 0 & 0 \\ i_{2,2}l_{2,3}l_{3,4}l_{4,1} & 0 & 0 & 0 \\ 0 & 0 & 0 & 0 \\ 0 & 0 & 0 & 0 \end{pmatrix},$$

where z was 2 because the loopback number was 2. We also performed the calculation for other wavelengths. Thus, $\boldsymbol{O}$ was calculated as follows.

$$\boldsymbol{O} = \sum_{q=1}^{4} \boldsymbol{O_q} = \begin{pmatrix} i_{1,1}l_{1,1} & i_{1,2}l_{1,2} & i_{1,3}l_{1,3} & i_{1,4}l_{1,4} \\ i_{2,4}l_{2,1} + i_{2,2}l_{2,3}l_{3,4}l_{4,1} & i_{2,1}l_{2,2} & 0 & i_{2,3}l_{2,4} \\ i_{3,3}l_{3,1} & i_{3,4}l_{3,2} & i_{3,1}l_{3,3} & 0 \\ 0 & i_{4,3}l_{4,2} & i_{4,4}l_{4,3} & i_{4,1}l_{4,4} \end{pmatrix}. \tag{15}$$

Consequently, the wavelength paths from nodes 2 to 3, from nodes 3 to 4, and from nodes 4 to 1 were relocated to the wavelength path from nodes 2 to 1 and the number of wavelength paths was increased twice. Thus, the transmission capacity between nodes 2 to 1 increased twice. We showed the justification on the result of path relocation. As shown in Table 1, the wavelength path corresponding to λ_2 in node 2 was inputted to In-2 in the AWGR and then it was outputted from Out-3. However, it was looped back to In-3 in the AWGR through the OSW corresponding to λ_2 in node 3 as the state of the OSW was C_{LB}. Subsequently, the looped back wavelength λ_2 was inputted to In-3 and routed to Out-4. In addition, looped back wavelength λ_2 was looped back to In-4 in the AWGR through the OSW corresponding to λ_2 in node 4 and routed to Out-1. Furthermore, there were no wavelength paths corresponding to λ_2 from nodes 2 to 3 and from nodes 3 to 4. It was confirmed that the elements that were 0 in Equation (15) agreed with the relationship

that did not have any wavelength path among the nodes. Based on this justification, the result of the calculation was the same as the result of confirming the routing table.

In the case of path capacities calculation, $\boldsymbol{O}$ is calculated as follows:

$$\boldsymbol{O} = \begin{pmatrix} 1 & 1 & 1 & 1 \\ 2 & 1 & 0 & 1 \\ 1 & 1 & 1 & 0 \\ 0 & 1 & 1 & 1 \end{pmatrix}.$$

Three paths did not exist, and the capacity between nodes 2 and 1 increased twice. In the case of margin calculation, it is important to define which optical power to assign to $i_{p,q}$ and which optical loss to assign to $l_{j,k}$. These can be clarified by considering what components pass through when the state of the OSW is $\mathrm{C_{LB}}$ and what components pass through when the state of the OSW is $\mathrm{C_{PT}}$. Here, the power after transmitting the signal from the L3SW passes through the MUX is $i_{p,q}$ and cumulative optical loss as it passes through fiber, AWGR, and MUX/DEMUX after passing through MUX is $l_{j,k}$. Table 2 shows the database of optical devices assumed in this AWG-STAR network. In this case, $i_{p,q}$, $l_{j,k}$, and $\min P$ were 1.5, -12.6, and -35.0 dBm, respectively. We have constructed an experimental network based on our proposal in [7] and developed a remote-control system in our laboratory to evaluate the performance of wavelength path relocation [10]. Furthermore, we have demonstrated extension of our network with semiconductor optical amplifier unit and showed solution when we cannot establish wavelength path due to too much optical loss [11]. The database in Table 2 is based on the average of multiple

TABLE 2. Optical loss database

Item	Value	Unit
Loss of AWGR	4.5	dB
Loss of MUX/DEMUX	1.5	dB
Loss of OSWs (WSSs)	0.6	dB
Loss of fibers	0.3	dB/km
Transmitting power of transceivers	+3.0	dBm
Minimum light reception power of transceivers	−35.0	dBm
Length of fibers	10	km

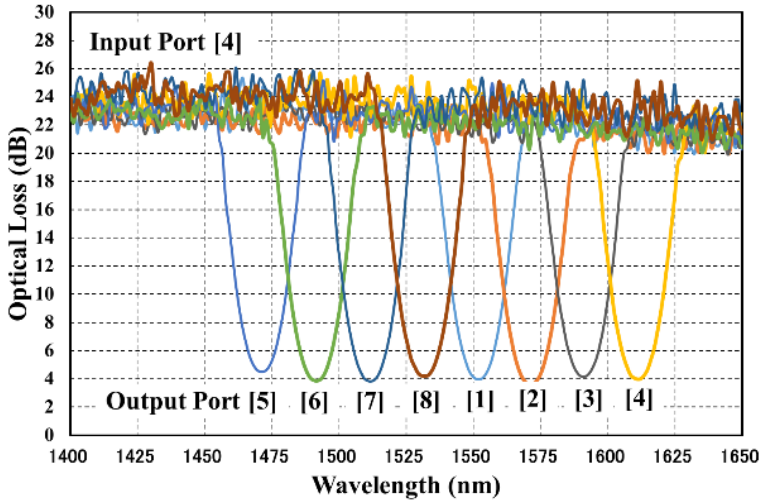

FIGURE 3. (color online) From input port 4 to other ports

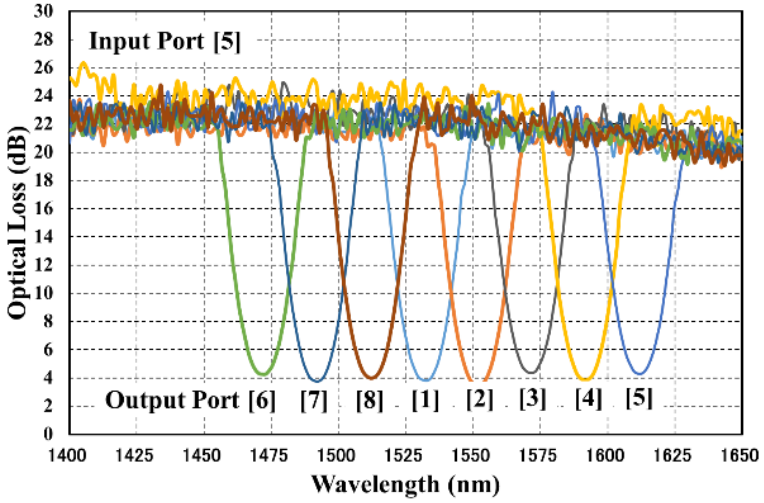

FIGURE 4. (color online) From input port 5 to other ports

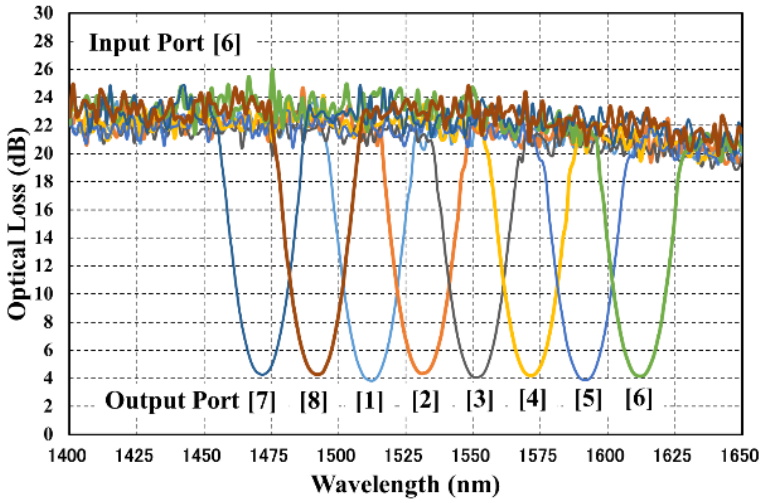

FIGURE 5. (color online) From input port 6 to other ports

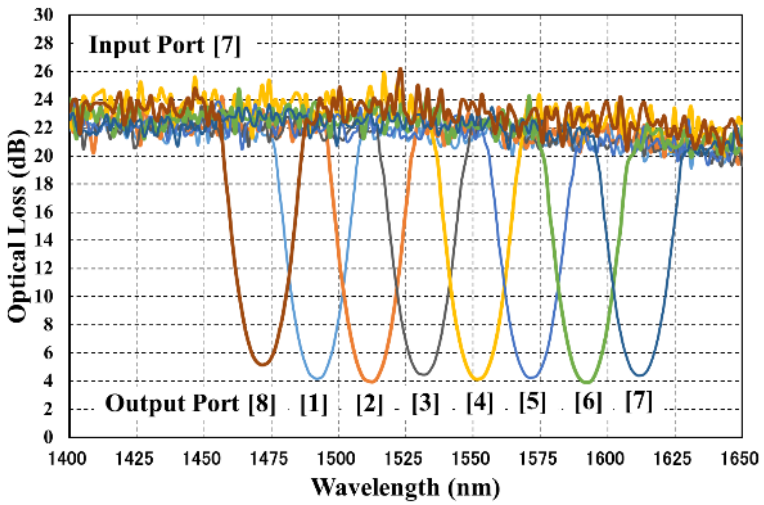

FIGURE 6. (color online) From input port 7 to other ports

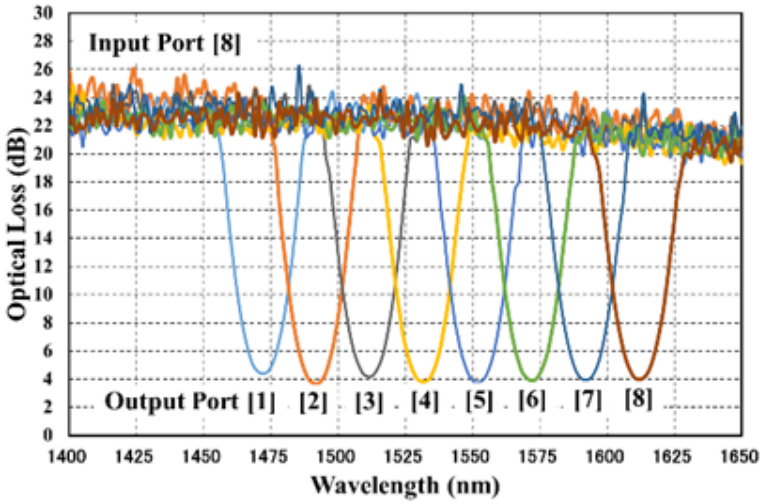

FIGURE 7. (color online) From input port 8 to other ports

measurements of optical loss values for optical components owned by our laboratory. Figures 3-7 show the results of the measurement for optical losses which are from an input port to other output ports of 8×8 AWGR in our laboratory. The results of input port 1, 2, and 3 were already reported in [9], so input ports 4 to 8 are shown in Figures 3-7. The database regarding AWGR in Table 2 is based on these results of measurements.

Thus, $\boldsymbol{O_2}$ corresponding to wavelength 7 was calculated as follows:

$$\boldsymbol{O_2} = \begin{pmatrix} 0 & i_{1,2}l_{1,2} & 0 & 0 \\ i_{2,2}l_{2,3}l_{3,4}l_{4,1} & 0 & 0 & 0 \\ 0 & 0 & 0 & 0 \\ 0 & 0 & 0 & 0 \end{pmatrix}$$

$$= \begin{pmatrix} 0 & 10^{\frac{1.5}{10}}10^{\frac{-12.6}{10}} & 0 & 0 \\ 10^{\frac{1.5}{10}}10^{\frac{-12.6}{10}}10^{\frac{-12.6}{10}}10^{\frac{-12.6}{10}} & 0 & 0 & 0 \\ 0 & 0 & 0 & 0 \\ 0 & 0 & 0 & 0 \end{pmatrix} \text{(mW)}$$

$$= 10\log_{10}\begin{pmatrix} 0 & 10^{\frac{1.5}{10}}10^{\frac{-12.6}{10}} & 0 & 0 \\ 10^{\frac{1.5}{10}}10^{\frac{-12.6}{10}}10^{\frac{-12.6}{10}}10^{\frac{-12.6}{10}} & 0 & 0 & 0 \\ 0 & 0 & 0 & 0 \\ 0 & 0 & 0 & 0 \end{pmatrix} \text{(dBm)}$$

$$= \begin{pmatrix} -\infty & -11.1 & -\infty & -\infty \\ -36.3 & -\infty & -\infty & -\infty \\ -\infty & -\infty & -\infty & -\infty \\ -\infty & -\infty & -\infty & -\infty \end{pmatrix} \text{(dBm)}$$

Thus, $\boldsymbol{M_2}$ was calculated as follows:

$$\boldsymbol{M_2} = \boldsymbol{O_2} - \min P = \begin{pmatrix} -\infty & 23.9 & -\infty & -\infty \\ -1.3 & -\infty & -\infty & -\infty \\ -\infty & -\infty & -\infty & -\infty \\ -\infty & -\infty & -\infty & -\infty \end{pmatrix} (\text{dBm})$$

As a result, $\boldsymbol{M_1}$, $\boldsymbol{M_2}$, $\boldsymbol{M_3}$, and $\boldsymbol{M_4}$ are calculated as follows:

$$\boldsymbol{M_1} = \begin{pmatrix} 23.9 & -\infty & -\infty & -\infty \\ -\infty & 23.9 & -\infty & -\infty \\ -\infty & -\infty & 23.9 & -\infty \\ -\infty & -\infty & -\infty & 23.9 \end{pmatrix}, \ \boldsymbol{M_2} = \begin{pmatrix} -\infty & 23.9 & -\infty & -\infty \\ -1.3 & -\infty & -\infty & -\infty \\ -\infty & -\infty & -\infty & -\infty \\ -\infty & -\infty & -\infty & -\infty \end{pmatrix},$$

$$\boldsymbol{M_3} = \begin{pmatrix} -\infty & -\infty & 23.9 & -\infty \\ -\infty & -\infty & -\infty & 23.9 \\ 23.9 & -\infty & -\infty & -\infty \\ -\infty & 23.9 & -\infty & -\infty \end{pmatrix}, \ \boldsymbol{M_4} = \begin{pmatrix} -\infty & -\infty & -\infty & 23.9 \\ 23.9 & -\infty & -\infty & -\infty \\ -\infty & 23.9 & -\infty & -\infty \\ -\infty & -\infty & 23.9 & -\infty \end{pmatrix}.$$

Therefore, the wavelength path from nodes 2 to 1 at λ_2 could not be established as the margin of the wavelength path was a negative value despite it being possible to establish the wavelength path from nodes 2 to 1 at λ_4. We would overlook this result and plan configuring unreachable path if we used the previous method [14] and calculated only path capacity. This was why the optical margin was important and we proposed a new calculation method.

In the second sample, we considered a situation where the states of the OSWs corresponding to λ_4 in node 2 and λ_2 in node 4 from $\mathrm{C_{PT}}$ to $\mathrm{C_{LB}}$. In this case, $\boldsymbol{S}$ and $\boldsymbol{I}$ were, respectively, expressed as

$$\boldsymbol{S} = \begin{pmatrix} 0 & 0 & 0 & 0 \\ 0 & 0 & 0 & 1 \\ 0 & 0 & 0 & 0 \\ 0 & 1 & 0 & 0 \end{pmatrix}, \ \boldsymbol{I} = \begin{pmatrix} i_{1,1} & i_{1,2} & i_{1,3} & i_{1,4} \\ i_{2,1} & i_{2,2} & i_{2,3} & 0 \\ i_{3,1} & i_{3,2} & i_{3,3} & i_{3,4} \\ i_{4,1} & 0 & i_{4,3} & i_{4,4} \end{pmatrix}.$$

In this instance, $\boldsymbol{D}$ was a 0 matrix and $\boldsymbol{O}$ was calculated as

$$\boldsymbol{O} = \sum_{q=1}^{4} \boldsymbol{O_q} = \begin{pmatrix} i_{1,1}l_{1,1} & i_{1,2}l_{1,2} & i_{1,3}l_{1,3} & i_{1,4}l_{1,4} \\ 0 & i_{2,1}l_{2,2} & i_{2,2}l_{2,3} & i_{2,3}l_{2,4} \\ i_{3,2}l_{3,4}l_{4,1} + i_{3,3}l_{3,1} + i_{3,4}l_{3,2}l_{2,1} & 0 & i_{3,1}l_{3,3} & 0 \\ 0 & i_{4,3}l_{4,2} & i_{4,4}l_{4,3} & i_{4,1}l_{4,4} \end{pmatrix} \tag{16}$$

In the path capacities calculation case, $\boldsymbol{O}$ is calculated as

$$\boldsymbol{O} = \begin{pmatrix} 1 & 1 & 1 & 1 \\ 0 & 1 & 1 & 1 \\ 3 & 0 & 1 & 0 \\ 0 & 1 & 1 & 1 \end{pmatrix}.$$

Four paths did not exist, and capacity between nodes 3 and 1 increased threefold. We showed the justification on the result of path relocation as same as the first example. As shown in Table 1, the wavelength path corresponding to λ_2 in node 3 was inputted to In-3 in the AWGR and then it was outputted from Out-4. However, it was looped back to In-4 in the AWGR through the OSW corresponding to λ_2 in node 4 as the state of the OSW was $\mathrm{C_{LB}}$. Subsequently, the looped back wavelength λ_2 was inputted to In-4 and routed to Out-1. In the same way, the wavelength path corresponding to λ_4 in node 3 was inputted

to In-3 in the AWGR and then it was outputted from Out-2. However, it was looped back to In-2 in the AWGR through the OSW corresponding to λ_4 in node 2 as the state of the OSW was C_{LB}. Subsequently, the looped back wavelength λ_4 was inputted to In-2 and routed to Out-1. Furthermore, no wavelength paths were corresponding to λ_2 from nodes 3 to 4 and corresponding to λ_4 from nodes 3 to 2. It was confirmed that the elements that were 0 in Equation (16) agreed with the relationship that did not have any wavelength path among the nodes. Based on this justification, the result of the calculation was the same as the result of confirming the routing table. Table 2 shows the database of optical devices assumed in this AWG-STAR network. In this example, $\boldsymbol{M_1}$, $\boldsymbol{M_2}$, $\boldsymbol{M_3}$, and $\boldsymbol{M_4}$ are, respectively, calculated as

$$\boldsymbol{M_1} = \begin{pmatrix} 23.9 & -\infty & -\infty & -\infty \\ -\infty & 23.9 & -\infty & -\infty \\ -\infty & -\infty & 23.9 & -\infty \\ -\infty & -\infty & -\infty & 23.9 \end{pmatrix}, \quad \boldsymbol{M_2} = \begin{pmatrix} -\infty & 23.9 & -\infty & -\infty \\ -\infty & -\infty & 23.9 & -\infty \\ 11.3 & -\infty & -\infty & -\infty \\ -\infty & -\infty & -\infty & -\infty \end{pmatrix},$$

$$\boldsymbol{M_3} = \begin{pmatrix} -\infty & -\infty & 23.9 & -\infty \\ -\infty & -\infty & -\infty & 23.9 \\ 23.9 & -\infty & -\infty & -\infty \\ -\infty & 23.9 & -\infty & -\infty \end{pmatrix}, \quad \boldsymbol{M_4} = \begin{pmatrix} -\infty & -\infty & -\infty & 23.9 \\ -\infty & -\infty & -\infty & -\infty \\ 11.3 & -\infty & -\infty & -\infty \\ -\infty & -\infty & 23.9 & -\infty \end{pmatrix}.$$

Therefore, both wavelength paths from nodes 3 to 1 at λ_2 and λ_4 could establish as the margin of the wavelength path was a positive value.

Consequently, we could express the wavelength path topology including transit nodes in the AWG-STAR network with loopback function employing a 4×4 AWG with the proposed matrix calculation and showed that the changes in path topology, in network capacity, and optical margins caused by the relocations could be derived. Furthermore, the matrix calculation can apply to the AWG-STAR network with loopback function, employing $N \times N$ AWGR and N optical switches in each node flexibly. In this case, more flexible relocation can be achieved but path topology is also more complex so that management of optical power is more important. We would overlook this result and plan configuring unreachable path if we used the previous method [14] and calculated only path capacity as shown in the first example.

4. **Conclusion.** We proposed a matrix calculation method that can calculate path topology and optical margins in an AWG-STAR network with a loopback function. Furthermore, we used a concrete example to illustrate the application of the proposed method using a 4×4 AWG-STAR network. The proposed method expressed network topology so that this method could also calculate network information based on topologies such as distance and latency and be helpful for a network controller that needs topology information. We would overlook unreachable path and plan configuring it if we used the previous method [14] and calculated only path capacity. The proposed method minimizes the operating expenses for complex networks by clarifying path relations among nodes. Consequently, we aimed to achieve automatic relocation and reduce operating expenses of the AWG-STAR network with a loopback function.

Acknowledgement. This work was supported by JSPS KAKENHI Grant Number 16K0 6306.

REFERENCES

[1] K. Jones, Enabling technologies for in-router DWDM interfaces for intra-data center networks, *Proc. of Optical Fiber Communication Conference*, 2019.

[2] M. Xu, J. Diakonikolas, E. Modiano and S. Subramaniam, A hierarchical WDM-based scalable data center network architecture, *Proc. of 2019 IEEE International Conference on Communications*, pp.1-7, 2019.

[3] G. Wang, D. G. Andersen, M. Kaminsky, K. Papagiannaki, T. E. Ng, M. Kozuch and M. Ryan, c-Through: Part-time optics in data centers, *Proc. of the ACM SIGCOMM 2010 Conference*, pp.327-338, 2010.

[4] N. Farrington, G. Porter, S. Radhakrishnan, H. H. Bazzaz, V. Subramanya, Y. Fainman, G. Papen and A. Vahdat, Helios: A hybrid electrical/optical switch architecture for modular data centers, *Proc. of the ACM SIGCOMM 2010 Conference*, pp.339-350, 2010.

[5] H. Liu, F. Lu, A. Forencich, R. Kapoor, M. Tewari, G. M. Voelker, G. Papen, A. C. Snoeren and G. Porter, Circuit switching under the radar with REACToR, *Proc. of the 11th USENIX Symposium on Networked Systems Design and Implementation*, pp.1-15, 2014.

[6] M. Ghobadi, R. Mahajan, A. Phanishayee, N. Devanur, J. Kulkarni, G. Ranade, P.-A. Blanche, H. Rastegarfar, M. Glick and D. Kilper, ProjecToR: Agile reconfigurable data center interconnect, *Proc. of 2016 ACM SIGCOMM Conference*, pp.216-229, 2016.

[7] M. Yamaguchi, R. Higashiyama, K. Toyonaga, O. Koyama and M. Yamada, AWG star-network with dynamically reconfigurable wavelength paths via node-side control, *Proc. of OSA Advanced Photonics for Communications*, 2014.

[8] R. Higashiyama, M. Yamaguchi, K. Toyonaga, O. Koyama and M. Yamada, Dynamic enhancement of internode transmission capacity in IP over AWG-STAR network, *Proc. of the 20th Asia-Pacific Conference on Communication*, pp.321-324, 2014.

[9] O. Koyama, M. Yamaguchi, H. Maruyama, T. Niihara and M. Yamada, Performance evaluation on wavelength path relocation via node-side control in AWG-STAR network, *ICIC Express Letters*, vol.11, no.2, pp.301-308, 2017.

[10] Y. Tomioka, T. Kojima, O. Koyama, H. Maruyama, T. Niihara and M. Yamada, Performance evaluation of wavelength path relocation with IoT devices in AWG-STAR network, *Proc. of the 22nd Opto-Electronics and Communications Conference*, 2017.

[11] Y. Ogura, O. Koyama, M. Yamaguchi, Y. Tomioka, S. Aso, K. Ota, K. Ikeda and M. Yamada, Experimental demonstration of wavelength path relocation using semiconductor optical amplifier unit in AWG-STAR with loop-back function, *Proc. of the 5th International Symposium on Extremely Advanced Transmission Technologies*, 2019.

[12] K. Oguchi, New notations based on the wavelength transfer matrix for functional analysis of wavelength circuits and new WDM networks using AWG-based star coupler with asymmetric characteristics, *Journal of Lightwave Technology*, vol.14, no.6, pp.1255-1263, 1996.

[13] A. Guo and J. Fu, Matrix analysis of wavelength transmission of arrayed waveguide grating multiplexer, *Microwave and Optical Technology Letters*, vol.30, no.4, pp.249-252, 2001.

[14] M. Yamaguchi, O. Koyama, H. Maruyama, T. Niihara and M. Yamada, Matrix representation for wavelength path relocation in AWG-STAR network with loopback function, *International Journal of Innovative Computing, Information and Control*, vol.12, no.3, pp.833-845, 2016.

[15] N. S. Bergano, F. W. Kerfoot and C. R. Davidsion, Margin measurements in optical amplifier system, *Photonics Technology Letters*, vol.5, no.3, pp.304-306, 1993.

[16] K. Oguchi, Network design method for wavelength routing networks, *Proc. of the 14th OptoElectronics and Communications Conference*, 2009.